THE JOURNAL OF BIOLOGICAL CHEMISTRY VOL. 286, NO. 5, pp. 3618–3629, February 4, 2011

Processing of Optineurin in Neuronal Cells*

Received for publication, August 16, 2010, and in revised form, November 4, 2010 Published, JBC Papers in Press, November 8, 2010, DOI 10.1074/jbc.M110.175810

Xiang Shen[‡], Hongyu Ying[‡], Ye Qiu[‡], Jeong-Seok Park[‡], Rajalekshmy Shyam[‡], Zai-Long Chi[§], Takeshi Iwata[§], and Beatrice Y. J. T. Yue[‡1]

From the [‡]Department of Ophthalmology and Visual Sciences, College of Medicine, University of Illinois, Chicago, Illinois 60612 and the [§]National Institute of Sensory Organs, National Hospital Organization Tokyo Medical Center, 152-8902 Tokyo, Japan

Optineurin is a gene linked to amyotrophic lateral sclerosis, Paget disease of bone, and glaucoma, a major blinding disease. Mutations such as E50K were identified in glaucoma patients. We investigated herein the involvement of ubiquitin-proteasome pathway (UPP) and autophagy, two major routes for protein clearance, in processing of optineurin in a retinal ganglion cell model line RGC5 and neuronal PC12 cells. It was found that the endogenous optineurin level in neuronal cells was increased by treatment of proteasomal inhibitor but not by autophagic and lysosomal inhibitors. Multiple bands immunoreactive to anti-ubiquitin were seen in the optineurin pulldown, indicating that optineurin was ubiquitinated. In cells overexpressing wild type and E50K optineurin, the level of the proteasome regulatory β5 subunit (PSMB5, indicative of proteasome activity) was reduced, whereas that for autophagy marker microtubule-associated protein 1 light chain 3 was enhanced compared with controls. Autophagosome formation was detected by electron microscopy. The foci formed after optineurin transfection were increased upon treatment of an autophagic inhibitor but were decreased by treatment of an inducer, rapamycin. Moreover, the level of optineurin-triggered apoptosis was reduced by rapamycin. This study thus provides compelling evidence that in a normal homeostatic situation, the turnover of endogenous optineurin involves mainly UPP. When optineurin is up-regulated or mutated, the UPP function is compromised, and autophagy comes into play. A decreased PSMB5 level and an induced autophagy were also demonstrated *in vivo* in retinal ganglion cells of E50K transgenic mice, validating and making relevant the *in vitro* findings.

Glaucoma is one of the leading causes of irreversible blindness worldwide (1) and is characterized by a progressive loss of retinal ganglion cells (RGCs)[2] and axons and distinctive cupping of the optic nerve head. The most common form of this disease, primary open angle glaucoma, is genetically heterogeneous, caused by several susceptibility genes and perhaps also environmental factors (1–4). Currently, a total of 14 chromosomal loci, designated as GLC1A to GLC1N, have been linked to primary open angle glaucoma. Three candidate genes identified so far include myocilin (GLC1A), optineurin (GLC1E), and WD40-repeat36 (GLC1G) (1–3). Among them, optineurin is linked principally to normal pressure or normal tension glaucoma (NTG), a subtype of primary open angle glaucoma (5). Optineurin mutations were noted to vary with ethnic background (6). The E50K mutation, found in Caucasian and Hispanic populations (6), seems to be associated with a more progressive and severe disease in NTG patients (7). Very recently, optineurin has also been linked to amyotrophic lateral sclerosis (8) and Paget disease of bone (9).

The human optineurin gene codes for a 577-amino acid protein that contains multiple coiled-coil domains and a C-terminal zinc finger (10). The optineurin protein from different species has high amino acid homology (11), and the amino acid 50 glutamic acid residue is conserved in mouse, rat, chicken, and cow (12). Optineurin is ubiquitously expressed in nonocular tissues such as the heart and brain (10) and in ocular tissues, including the retina, trabecular meshwork, and nonpigmented ciliary epithelium (9). In the retina, RGCs are immunolabeled with a high intensity (12, 13).

Optineurin shares a 53% amino acid homology with NF-κB essential modulator and was identified as an NF-κB essential modulator-related protein (14). Recently, optineurin has been shown to be a negative regulator of NF-κB (15). Like NF-κB essential modulator, optineurin has a polyubiquitin-binding region in the sequence, and it binds Lys-63 linked polyubiquitinated chains (16). Optineurin has in addition been demonstrated to interact with itself to form homo-hexamers (17). It also interacts with proteins, including myosin VI, Rab8, and transferrin receptor. Super molecular complexes are detected, and granular structures termed foci are formed when optineurin is overexpressed or E50K mutated (17, 18).

Proper processing of cellular proteins is of vital importance. In eukaryotic cells, the ubiquitin-proteasome pathway (UPP) and autophagy are two major routes for protein clearance (19–21). Proteasomes predominantly degrade, in a specific manner, short lived nuclear and cytosolic proteins. The bulk degradation of long lived cytoplasmic proteins or organelles is mediated largely by autophagy. Proteins can also be degraded through the autophagy-independent endosome-lysosome system.

Protein degradation via UPP is a temporally controlled and tightly regulated process that involves covalent linking of a

* This work was supported, in whole or in part, by National Institutes of Health Grants EY018828, EY005628, and EY003890 from NEI (to B. Y. J. T. Y.) and Core Grant EY01792. This work was also supported by Ministry of Health, Labor, and Welfare and Ministry of Education, Culture, Sports, Science, and Technology of Japan (to T. I.).

[1] To whom correspondence should be addressed: Dept. of Ophthalmology and Visual Sciences, University of Illinois, 1855 West Taylor St., Chicago, IL 60612. Fax: 312-996-7773; E-mail: beatyue@uic.edu.

[2] The abbreviations used are: RGC, retinal ganglion cell; DOX, doxycycline; IP, immunoprecipitation; LCT, lactacystin; 3-MA, 3-methyladenine; NTG, normal tension glaucoma; OPTN, optineurin; UPP, ubiquitin-proteasome pathway.

single or multiple molecules of ubiquitin to a target protein. The ubiquitinated protein is then marked for degradation by the multisubunit 26 S proteasome complex. The proteolytic core of the complex, the 20 S proteasome, contains multiple peptidase activities that include chymotrypsin-like, postglutamyl peptidase or caspase-like and trypsin-like activities. Ubiquitination has been shown to be a pivotal player in regulating a host of cellular processes, including cell cycle control, differentiation, and quality control (22). It is important not only in cellular homeostasis in tissues/organs, including the nervous system, but also in degradation of misfolded and aberrant proteins.

Autophagy is an evolutionally conserved mechanism responsible for the nonselective bulk degradation of long lived proteins and cytoplasmic recycling of organelles during development, tissue homeostasis, and environmental stress such as starvation or amino acid depletion (23, 24). There are three types of autophagy as follows: macroautophagy, chaperone-mediated autophagy, and microautophagy. Among them, macroautophagy (hereafter referred to as autophagy) is the one mediated by the organelle termed autophagosome. Chaperone-mediated autophagy involves the direct translocation of cytosolic proteins across the lysosomal membrane, which requires protein unfolding by chaperone proteins. Microautophagy involves inward invagination of lysosomal membrane, which delivers a small portion of cytoplasm into the lysosomal lumen.

Autophagy begins with the formation of double membrane-bounded autophagosomes (25–27), which then fuse with lysosomes to form autolysosomes. The contents of autolysosomes are finally degraded by acidic lysosomal hydrolases and the degraded products are transported back to the cytoplasm. Autophagy has been shown to play a role in organelle turnover, cancer cell biology, aging, and neurodegenerative disorders (23, 28–30).

In this study, we determined the involvement of UPP and autophagy in processing of the endogenous optineurin in RGC5 cells, a neuronal cell type recently shown to be of mouse origin (31) and an established model for RGCs (31, 32), as well as neuronal rat adrenal pheochromocytoma PC12 cells (33). The processing of overexpressed wild type optineurin and E50K mutant protein was also studied to test the hypothesis that, similar to other neurodegenerative diseases, UPP function is compromised and autophagy is induced with elevated level or mutation of aggregate-prone optineurin.

EXPERIMENTAL PROCEDURES

Cell Lines—RGC5 cells were obtained from the University of Illinois, Chicago, Ophthalmology Departmental Core Facility, deposited by Dr. Paul Knepper (34) and originally from Dr. Neeraj Agarwal, North Texas Health Science Center, Fort Worth, TX (31). PC12 cells were purchased from American Type Culture Collection (Manassas, VA). The cells were cultured in serum-containing complete medium as described previously (18, 35).

In some experiments, RGC5 cells were treated with tumor necrosis factor-α (TNF-α, 100 ng/ml, R & D Systems, Minneapolis, MN) or interferon-γ (IFN-γ, 20 ng/ml, R & D Systems) for 24 h. Both have been shown to elevate the level of optineurin (14, 15, 36). Tetracycline-regulated (Tet-On) wild type optineurin ($OPTN_{WT}$)-green fluorescence protein (GFP)-inducible stable RGC5 cell line was established as described previously (17). Tet-On-inducible E50K optineurin ($OPTN_{E50K}$)-GFP RGC5 cell line was, in addition, created following the same procedures and strategies. The only exception was that the $OPTN_{WT}$-GFP fragment was replaced with $OPTN_{E50K}$-GFP during the first cloning step (17). The cells were maintained in DMEM complete medium with 10% Tet system certified fetal bovine serum (Clontech), essential and nonessential amino acids, and antibiotics. To induce expression of $OPTN_{WT}$-GFP and $OPTN_{E50K}$-GFP, cells were treated for 16 h with doxycycline (DOX, 1 μg/ml) (Clontech) in DMEM complete medium.

DNA Constructs—Optineurin expression vectors pTarget-$OPTN_{WT}$, pTarget-FLAG-$OPTN_{WT}$, p$OPTN_{WT}$-EGFP, p$OPTN_{WT}$-DsRed, as well as pTarget-$OPTN_{E50K,}$ p$OPTN_{E50K}$-GFP, and p$OPTN_{E50K}$-DsRed were constructed as described previously (18). Transient transfection was performed using Lipofectamine LTX and Plus reagent (Invitrogen) for 20–48 h according to the manufacturer's protocol.

Western Blotting—To examine the effects of various inhibitors on levels of the endogenous optineurin, RGC5 and PC12 cells in 6-well plates (300,000 cells/well) were treated for 16 h with vehicle dimethyl sulfoxide (DMSO) or H_2O, proteasomal inhibitors lactacystin (LCT, 1 μM) and epoxomicin (5 μM), autophagic inhibitor 3-methyladenine (3-MA, 5 mM), lysosomal inhibitor NH_4Cl (1 mM), or autophagic inducer rapamycin (2 μM). LCT is a proteasomal inhibitor, but it also inhibits enzymes such as cathepsin A. Epoxomicin, on the other hand, is a potent and specific proteasomal inhibitor. 3-MA inhibits class III phosphatidylinositol 3-kinase (PI3K) that is essential for autophagosome formation, as well as other classes of PI3K. It is used as an effective and selective drug to inhibit autophagy degradation. At 5 mM, it has no detectable effects on other proteolytic pathways (27). NH_4Cl is a lysosomotropic weak base that blocks the intralysosomal degradation of macromolecules via inhibition of the acidification of the endosome-lysosome system. It does not affect enzyme activities.

The cells were lysed with lysis buffer (250 mM NaCl, 50 mM Tris/HCl, pH 7.5, 5 mM EDTA, 0.5% Nonidet P-40) supplemented with protease inhibitor mixture (Sigma). Protein concentration was determined by bicinchoninic acid protein assay (Pierce). Total cell lysate was then subjected to SDS-PAGE under reducing conditions. The proteins were transferred to nitrocellulose membrane, and the level of endogenous optineurin was assessed by Western blotting using rabbit anti-C-terminal optineurin (1:1000, Cayman Chemical). The membrane was also immunoblotted with polyclonal anti-glyceraldehyde 3-phosphate dehydrogenase (GAPDH) (1:5000, Trevigen, Gaithersburg, MD) for loading control. Immunoreactive protein bands were detected by chemiluminescence using SuperSignal substrate (Pierce). Densitometry was performed. The band intensity of the endogenous optineurin was normalized to that of GAPDH.

For levels of proteasome regulatory β5 subunit (PSMB5) that is responsible for the chymotrypsin-like activity of the proteasome (37) and an established autophagic marker microtubule-associated protein 1 light chain 3 (LC3) (25), RGC5 and PC12 cells were transfected for 20 h with pTarget empty vector, pTarget-$OPTN_{WT}$, or pTarget-$OPTN_{E50K}$. Total lysate was subject to SDS-PAGE, and levels of PSMB5, LC3, and GAPDH were assessed by immunoblotting using polyclonal rabbit anti-PSMB5 (1:1000, Abcam, Cambridge, MA), monoclonal anti-LC3 (1:1000, Enzo Life Sciences, Farmingdale, NY), and rabbit anti-GAPDH (1:5000).

Immunoprecipitation (IP)—Lysates from RGC5 cells untreated or treated with 1 μM LCT for 16 h were immunoblotted using polyclonal anti-optineurin or monoclonal anti-ubiquitin (1:2000, Biomol, Enzo Life Sciences). Lysates were also immunoprecipitated with rabbit anti-C-terminal optineurin or rabbit normal IgG (negative control) using the Catch and Release kit (Millipore, Billerica, MA). The proteins pulled down were subjected to SDS-PAGE under reducing conditions. The ubiquitinated proteins were detected with mouse anti-ubiquitin antibody.

Fluorescence Microscopy and Immunohistochemistry—RGC5 and PC12 cells were transfected for 20 h with pEGFP-N1 (mock control), $pOPTN_{WT}$-EGFP, or $pOPTN_{E50K}$-EGFP. The cells were subsequently treated for 24 or 48 h with autophagic inhibitor 3-MA (5 mM) or overnight with rapamycin (2 μM). The cells were fixed, and images were acquired.

For immunofluorescence, the cells were fixed after transfection or treatments, and single or double stained with rabbit anti-optineurin (1:100), rabbit anti-PSMB5 (1:100), or rabbit (MBL International, Woburn, MA) or mouse anti-LC3 (1:100). FITC-goat anti-rabbit IgG, Cy3-goat anti-rabbit IgG, or Cy3-goat anti-mouse IgG (1:200, Jackson ImmunoResearch, West Grove, PA) was used as the secondary antibody. The slides were mounted in Vectashield (Vector Laboratories, Burlingame, CA) with 4′,6-diamidino-2-phenylindole (DAPI).

Photography was carried out using a 63× oil objective on an Axioscope (Carl Zeiss MicroImaging, Thornwood, NY) with the aid of Metamorph software (Molecular Devices, Downingtown, PA). In some experiments, confocal microscopic analysis was performed on a Leica SP2 confocal system (Leica Microsystems, Bannockburn, IL) using the Leica confocal software following sequential scanning to minimize the bleed through.

GFP^u Reporter Assay—To visualize the change of proteasome activity by optineurin transfection, a GFP^u reporter plasmid (American Type Culture Collection) was used. It is a designer reporter consisting of a short 16-amino acid degron CL1 (a substrate for UPP) fused to the C terminus of GFP (38, 39). For GFP^u reporter assay, cells co-transfected with GFP^u and pDsRed empty vector (mock control), $pOPTN_{WT}$-DsRed, or $pOPTN_{E50K}$-DsRed for 24 h were examined by confocal microscopy. Images were captured after sequential scanning, and the intensity of green fluorescence in at least 60 red fluorescent-transfected cells was quantified.

Transmission Electron Microscopy—RGC5 cells transfected for 20 h to express GFP, $OPTN_{WT}$-GFP, or $OPTN_{E50K}$-GFP were fixed in 2.5% glutaraldehyde, 2% paraformaldehyde in sodium cacodylate buffer, pH 7.4, postfixed in osmium tetroxide, and embedded in Epon resin. Ultra thin sections (70 nm) were counterstained with uranyl acetate and lead citrate and observed under a JEOL JEM-1220 transmission electron microscope.

For immunogold experiments, inducible cells without or with DOX treatment were fixed at 4 °C in 4% paraformaldehyde, 0.1% glutaraldehyde, in phosphate-buffered saline, pH 7.4, for 2 h and sequentially dehydrated in ethanol solutions and embedded in LR-White resin. Sections (90 nm) mounted on 200-mesh nickel grids were blocked and then incubated with polyclonal anti-GFP (1:100, for wild type or E50K optineurin-GFP) and monoclonal anti-LC3 (1:50). The secondary antibodies used were 25-nm colloid gold-conjugated goat anti-rabbit IgG and 10-nm gold-conjugated goat anti-mouse IgG (1:25, Jackson ImmunoResearch).

Apoptosis Assay—Apoptosis was evaluated by the Biomol CV-caspase 3/7 detection kit (Enzo Life Sciences) that utilizes the fluorophore, cresyl violet, coupled to the C terminus of the optimal tetrapeptide recognition sequences for caspase 3/7, DEVD ($CR(DEVD)_2$). Cleavage of the target sequences by activated enzymes yields red fluorescence throughout the cell, indicative of apoptotic activity. RGC5 and PC12 cells on glass chamber slides were transiently transfected for 48 h to express GFP, or wild type, or E50K optineurin-GFP. Cells were incubated with $CR(DEVD)_2$ for 60 min after treatment with rapamycin for 30 h. The untreated control did not receive rapamycin treatment. The slides were mounted in Vectashield with DAPI, which stained nuclei of all transfected and nontransfected cells.

The total number of DAPI-stained transfected cells (green) and the number of $CR(DEVD)_2$-stained transfectants (displaying both green and red fluorescence) in 20 of randomly selected 10× fields were counted (40). The percentage of caspase 3/7-positive apoptotic cells in ~100 transfectants (number of green and red cells/number of green only cells) was calculated. The experiments were repeated three times. Statistical analysis was performed using Student's *t* tests.

Transgenic Mice—The E50K transgenic mice were generated as described previously (41). All the experiments using mice were performed in accordance with the Association for Research in Vision and Ophthalmology statement for the Use of Animals in Vision Research.

The intraocular pressure of the transgenic mice was measured using an impact-rebound tonometer (Colonial Medical Supply, Franconia, NH) and optical interferometry tonometer (FISO Technologies, Quebec, Canada). Optic disk imaging and light microscopic histopathological examination of the optic nerve were carried out. Paraffin sections of retinal tissues were prepared for TUNEL assay (39). Sections (5 μm) from 12-month-old normal and transgenic mice were deparaffinized and stained in parallel with hematoxylin and eosin, monoclonal anti-TUJ1 (anti-βIII-tubulin, 1:400, Covance, Princeton, NJ) to highlight RGC layer (42), or polyclonal anti-optineurin (1:100), anti-PSMB5 (1:250), or anti-LC3 (1:200). Qdot 655 goat anti-mouse or rabbit IgG (1:100, Invitrogen) was used as the secondary antibody. The slides were mounted

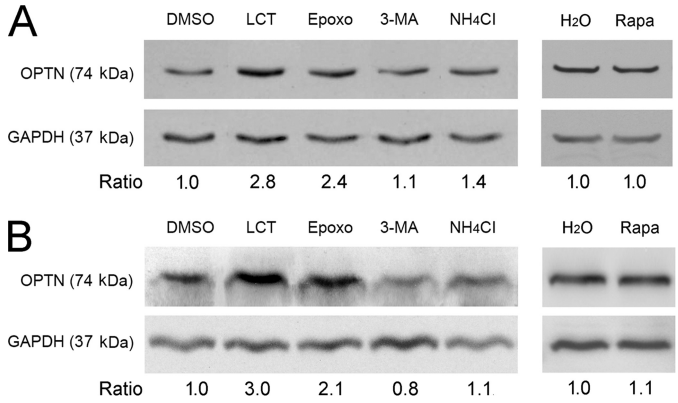

FIGURE 1. **Effects of proteasomal, autophagic, and lysosomal inhibitors on levels of the endogenous optineurin in RGC5 (*A*) and PC12 (*B*) cells.** Cells were treated for 16 h with vehicle DMSO or H_2O, or proteasomal (lactacystin) and epoxomicin (*Epoxo*)), autophagic (*3-MA*), or lysosomal (NH_4Cl) inhibitors. In a separate experiment, cells were also treated with rapamycin (*Rapa*) or vehicle (H_2O) for 16 h. Proteins (25 μg) in cell lysates were immunoblotted with anti-optineurin or anti-glyceraldehyde 3-phosphate dehydrogenase (*GAPDH*). Densitometry was performed. The optineurin/GAPDH relative to the DMSO or H_2O control ratios are presented.

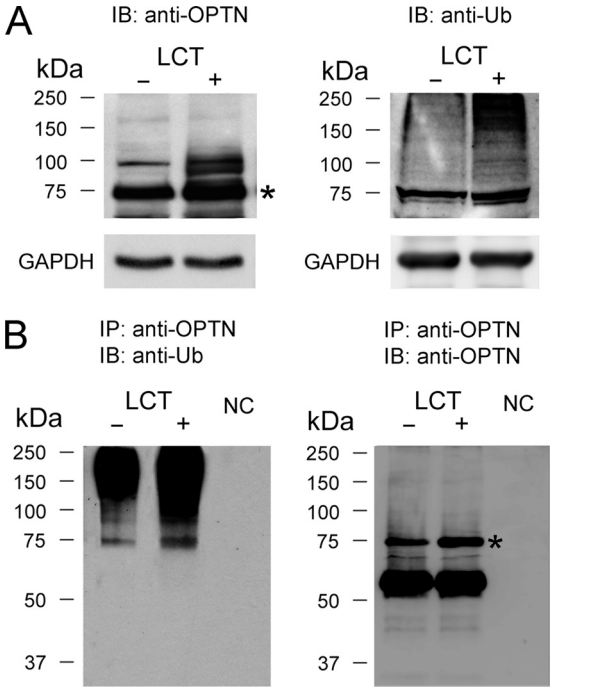

FIGURE 2. *A,* total lysates from RGC5 cells without or with treatment of lactacystin (*LCT*, 1 μM, 16 h) were immunoblotted (*IB*) with polyclonal anti-optineurin (*anti-OPTN, left panel*), anti-GAPDH, or monoclonal anti-ubiquitin (*anti-Ub, right panel*). *B,* total lysates from RGC5 cells without or with the LCT treatment were immunoprecipitated (*IP*) with rabbit anti-OPTN polyclonal antibody or normal rabbit IgG (as a negative control, *NC*) followed by immunoblotting (*IB*) with mouse anti-Ub monoclonal antibody. Optineurin pulldown by rabbit anti-OPTN, but not the rabbit IgG control, showed multiple bands immunoreactive to anti-ubiquitin (*left panel*). The intensity of the ubiquitin-positive bands was enhanced by prior LCT treatment. The same blot was also probed with anti-OPTN (*right panel*) to verify the IP procedure. *, the 74-kDa optineurin band.

in Vectashield, examined under Axioscope, and photographed. In some experiments, sections from 4- and 8-month-old mice were prepared and immunostained with anti-optineurin, anti-PSMB5, and anti-LC3. For EM, 12-month-old mouse eyes were fixed in 2.5% glutaraldehyde, 2% paraformaldehyde in phosphate buffer. The retinas were dissected out and the tissues were postfixed in 1% osmium tetroxide, sequentially dehydrated, and embedded in Spurr's resin. Thin sections (90 nm) were cut and stained for examination under JEOL 1200 EX transmission electron microscope.

RESULTS

Endogenous Optineurin Level in RGC5 and PC12 Cells—Cells were treated with proteasomal, autophagic, and lysosomal inhibitors. As can be seen in Fig. 1, the endogenous optineurin level in both RGC5 and PC12 cells was increased by 2–3-fold upon treatment with proteasomal inhibitors, LCT and expoxomicin, but only by 1.1–1.4-fold with autophagic and lysosomal inhibitors. Rapamycin, an autophagic inducer, did not alter the optineurin level, supporting the 3-MA results that autophagy has a minimal role in the processing of the endogenous optineurin.

Optineurin Is Ubiquitinated—Lysates from RGC5 cells were immunoprobed for optineurin and ubiquitin. Consistent with results from Fig. 1, the level of optineurin was increased upon treatment of LCT. Also seen were higher molecular weight bands with stronger intensities in LCT-treated samples (Fig. 2*A*, *left panel*). Meanwhile, LCT treatment, as anticipated, resulted in an enhanced level of total ubiquitinated proteins in cell lysates (Fig. 2*A*, *right panel*).

Lysates were in addition immunoprecipitated with polyclonal anti-optineurin and immunoprobed with monoclonal anti-ubiquitin. Multiple bands immunoreactive to anti-ubiquitin were observed in the immunoprecipitated protein pool, indicating that the endogenous optineurin in RGC5 cells was ubiquitinated (Fig. 2*B*, *left panel*). The intensity of the ubiquitin-positive bands was enhanced by prior LCT treatment. The same blot was also probed with anti-optineurin to verify the IP procedure (Fig. 2*B*, *right panel*).

Optineurin Foci Formation—After transfection, the overexpressed optineurin-GFP fusion protein distributed diffusely in the cytoplasm of RGC5 and PC12 cells with dots or granular structures observed most notably near the nucleus (Fig. 3). These structures, referred to as foci, were also observed previously in human retinal pigment epithelial and trabecular meshwork cells (18). Foci formation in addition was noted in cells after transfection to overexpress E50K optineurin-GFP. The number and the size of the E50K-GFP foci were greater than those of the wild type (Fig. 3), as was reported previously in retinal pigment epithelial cells (18).

Reduced Proteasome Activity in Optineurin Overexpressing Cells—RGC5 cells transfected for 20 h to express wild type and E50K optineurin-GFP were immunostained for PSMB5 as an indication of proteasome activity (37). The staining intensity in green optineurin-overexpressing RGC5 cells was much reduced compared with mock controls and nontransfected cells (Fig. 4*A*). Western blot analyses indicated that the PSMB5 protein level was decreased (0.36 ± 0.10 and 0.30 ± 0.14, respectively, $n = 3$, $p < 0.002$) as the optineurin level was increased by 8–10-fold upon transfection of pTarget-wild type and E50K optineurin (Fig. 4*B*). Similar alterations were also observed in PC 12 cells (data not shown).

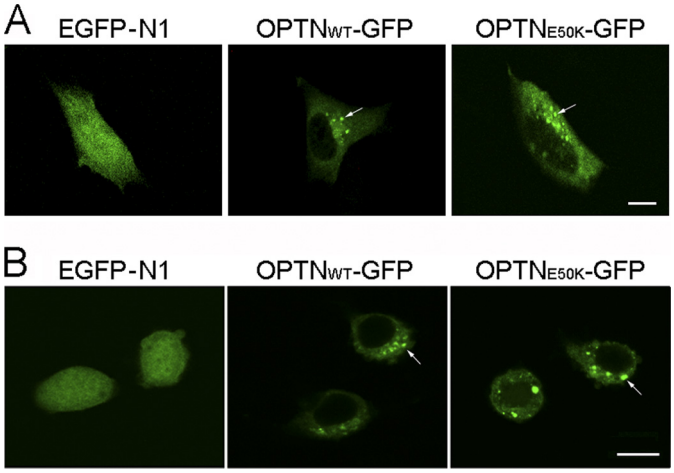

FIGURE 3. **Foci formation in RGC5 (*A*) and PC12 (*B*) cells after 20 h of transfection with pEGFP-N1 (mock control), pOPTN$_{WT}$-GFP, and pOPTN$_{E50K}$-GFP to express GFP, wild type, and E50K optineurin-GFP.** The optineurin-GFP fusion proteins distributed diffusely in the cytoplasm of RGC5 and PC12 cells with dots or granular structures (*arrows*) observed most notably near the nucleus. These structures are referred to as foci. *Scale bar,* 10 μm.

The cells were subsequently co-transfected with pOPTN$_{WT}$-DsRed and GFP^u reporter plasmid. This ubiquitin proteasome system reporter has been shown to be degraded in mammalian cells in an ubiquitin-dependent manner (38, 39). Proteasomal inhibitors such as LCT, but not other protease inhibitors, increased the steady state level of GFP^u (39). Its fluorescence readout and dependence on ubiquitin thus make GFP^u a simple and reliable tool (30). Results shown in Fig. 4, *C* and *D,* revealed that the GFP^u green fluorescence was increased, indicating a lowered proteasome activity in cells transfected with pOPTN$_{WT}$-DsRed compared with those of DsRed control and nontransfected cells. A decreased proteasome activity was also seen in cells transfected with pOPTN$_{E50K}$-DsRed (Fig. 4*C*).

Induction of Autophagy in Optineurin Overexpressing Cells—Following optineurin transfection, RGC5 (Fig. 5) and PC12 (data not shown) cells were stained for the autophagic marker LC3. The intensity of LC3 staining in optineurin-transfected green cells was found stronger than that seen in mock controls and nontransfected cells (Fig. 5*A*). Partial co-

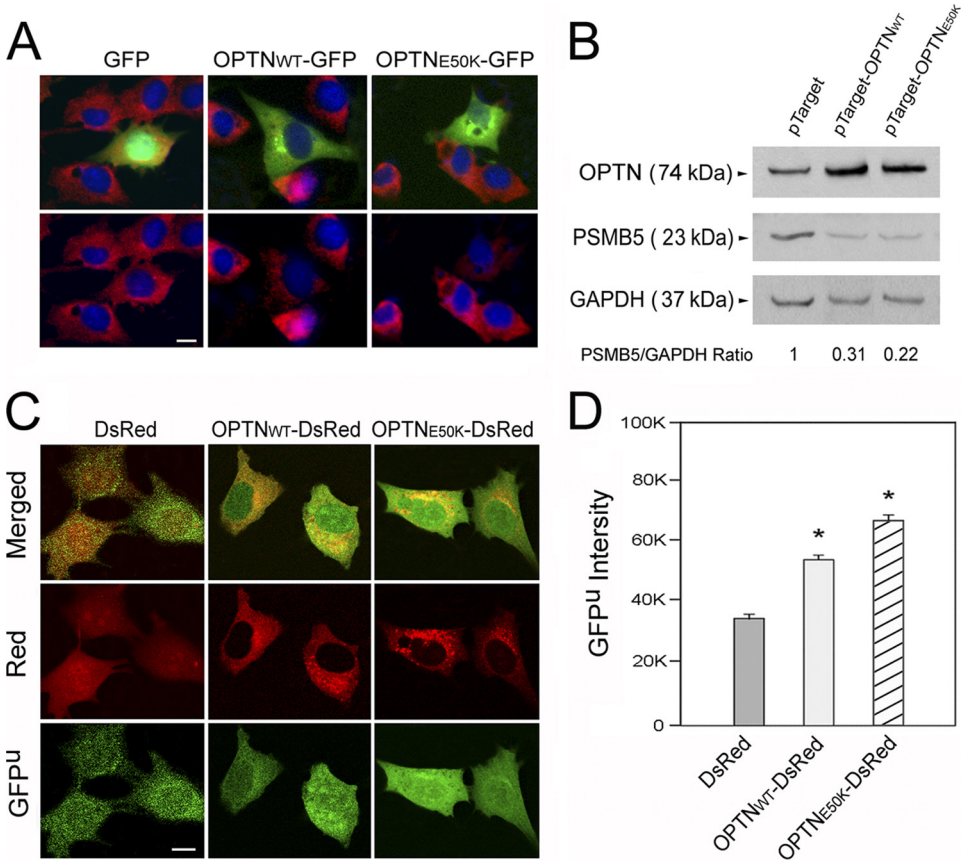

FIGURE 4. *A,* PSMB5 immunostaining (in *red*) in RGC5 cells. The cells were transfected for 20 h to express GFP, OPTN$_{WT}$-GFP, or OPTN$_{E50K}$-GFP. All transfectants displayed green fluorescence. Note a reduced PSMB5 staining intensity in optineurin-GFP-expressing green cells compared with GFP-expressing or nontransfected cells. The reduction was more striking with the E50K mutation than the wild type. *Scale bar,* 10 μm. *B,* Western blotting for PSMB5 protein level. RGC5 cells were transfected for 20 h with pTarget, pTarget-OPTN$_{WT}$, or pTarget-OPTN$_{E50K}$. Total lysate was subject to SDS-PAGE and immunoblotting (*IB*) using polyclonal rabbit anti-optineurin, anti-PSMB5, or anti-GAPDH. The optineurin (*OPTN*) level, normalized to that of GAPDH, was increased by 9.8- and 7.5-fold, respectively, after wild type and E50K optineurin-GFP transfection. The PSMB5/GAPDH relative to the GFP control ratios are presented. Similar results were also obtained with PC12 cells (data not shown). *C,* GFP^u reporter assay. RGC5 cells were co-transfected with GFP^u and pDsRed, pOPTN$_{WT}$-DsRed, or pOPTN$_{E50K}$-DsRed for 20 h. The transfected cells displaying both green and red fluorescence were examined by confocal sequential analyses. The loss of GFP^u green fluorescence is an indication of proteasome activity. The fluorescence intensity from GFP^u is thus inversely correlated to the proteasome activity. *Scale bar,* 10 μm. *D,* intensity of green fluorescence from GFP^u in red fluorescent-transfected cells was quantified. Results are presented as mean $\pm$ S.E. ($n > 60$) per transfected cells. The higher the value, the lower is the proteasome activity. *, $p < 0.0001$ compared with DsRed controls.

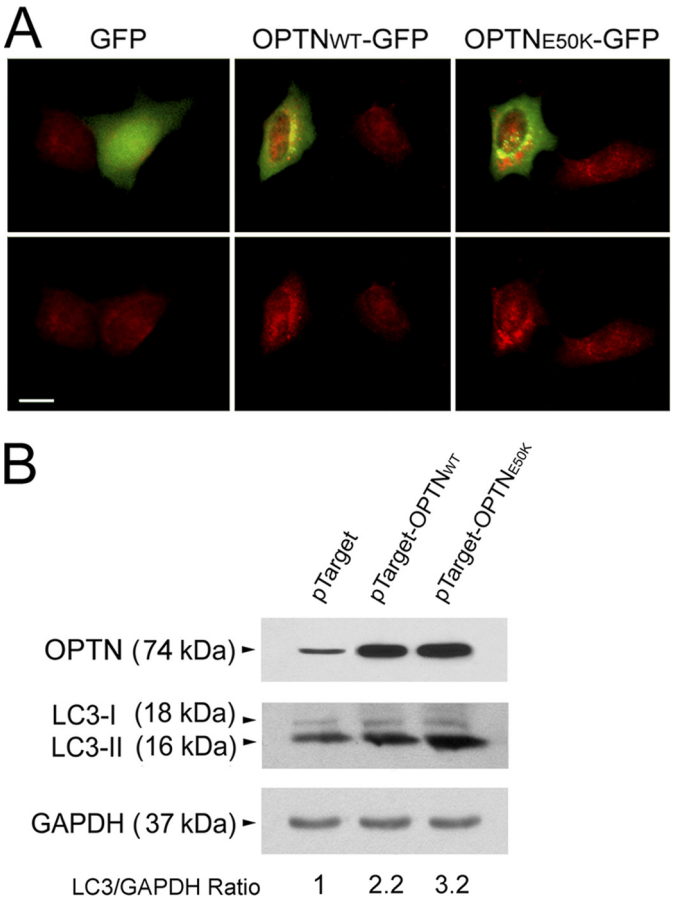

FIGURE 5. *A,* LC3 immunostaining in transfected RGC5 cells. The cells transfected for 20 h to express GFP, $OPTN_{WT}$-GFP, or $OPTN_{E50K}$-GFP were stained with rabbit anti-LC3 in *red*. The GFP and LC3 merged images are presented. Note an increased LC3 staining in optineurin-transfected green cells. The optineurin foci (*green*) and LC3 (*red*) were co-localized partially in the perinuclear region in *yellow*. *Bar,* 10 μm. *B,* Western blotting for LC3 protein level. RGC5 cells were transfected for 20 h with pTarget, pTarget-$OPTN_{WT}$, or pTarget-$OPTN_{E50K}$. Total lysate was subject to SDS-PAGE and immunoblotting (*IB*) using rabbit anti-optineurin, mouse anti-LC3, or rabbit anti-GAPDH. Both LC3-I and LC3-II protein bands were detected. The OPTN level, normalized to that of GAPDH, was increased by 11.5- and 12.3-fold, respectively, after wild type and E50K optineurin transfection. The LC3/GAPDH relative to the pTarget control ratios are presented. Similar alterations were also observed in PC12 cells (data not shown).

localization between optineurin foci and LC3 staining was observed.

LC3 exists in two forms. LC3-I (18 kDa) is cytosolic and LC3-II (16 kDa) is lipidated (conjugated to phosphatidylethanolamine) which is inserted into the membrane. The amount of LC3-II is correlated with the extent of autophagosome formation, and increasing levels of LC3-II on immunoblots have been used to document induction of autophagy (27). In RGC5 cells, the level of LC3 protein, especially the active LC3-II form, was found substantially increased (2.4 ± 0.4 and 2.7 ± 0.5 respectively, $n = 5$, $p < 0.002$) by Western blotting upon overexpression of wild type and E50K optineurin (Fig. 5*B*).

In separate experiments, RGC5 cells were treated with TNF-α and IFN-γ for 24 h. The optineurin level was increased by ~2-fold, as was reported previously (14, 15, 36). Foci formation was not apparent, but the PSMB5 level was found reduced by 40–60%, and the LC3-II level was elevated by 1.9–2.5-fold (Fig. 6). Similar PSMB5 and LC3 alterations were also observed in inducible cell lines when wild type and E50K optineurin-GFP levels were induced by 10–12-fold, and foci were formed upon DOX treatment (data not shown). It is of note that the overexpressed or up-regulated optineurin levels seen in Figs. 4–6 are not the expression levels but rather the stationary state levels set by expression and degradation. The resulting level depends not only on the translational increase but also on the maximum ability of the cell to degrade the excess proteins. This indicates that the transient overexpression might be much higher than 10 times but could be regulated somewhat by the autophagic degradation process.

Furthermore, electron dense as well as electron-light double or multiple membrane autophagosome- and autolysosome-like structures or vesicles (43, 44) were prominently observed by electron microscopy in RGC5 cells after optineurin transfection (Fig. 7*A*, *panels a–c*). These structures were rarely detected in GFP control (Fig. 7*A, panel d*) and nontransfected (data not shown) cells.

Autophagosome-like structures were also observed in inducible wild type (data not shown)- and E50K (Fig. 7*B*, *panels a* and *b*)-GFP-expressing cells following DOX induction but not in noninduced cells (Fig. 7*B, panel b, inset*). Immunogold studies showed co-localization of E50K optineurin-GFP and LC3 in autophagosome-like structures (Fig. 7*B*, *panels c* and *d*).

Optineurin Foci Formation Is Regulated by Autophagy—RGC5 (Fig. 8, *A* and *B*) and PC12 (data not shown) cells transfected with pOPTN$_{WT}$-GFP and/or pOPTN$_{E50K}$-GFP for 20 h were treated with 3-MA or rapamycin for 24 or 48 h. The 3-MA-treated cells showed more optineurin wild type foci formation compared with the untreated controls (Fig. 8*A*), and the foci enhancement was more dramatically seen at the 48-h time point. The rapamycin-treated cells, on the other hand, showed less foci formation compared with the untreated group in both pOPTN$_{WT}$-GFP and pOPTN$_{E50K}$-GFP transfectants (Fig. 8*B*), suggesting that the overexpressed optineurin was cleared, at least in part, via the autophagy pathway.

Rapamycin Treatment Reduces the Level of Apoptosis Induced by Overexpressed Optineurin—RGC5 (Fig. 8*C*) and PC12 (data not shown) cells were transiently transfected to express GFP alone, wild type or E50K optineurin-GFP followed by treatment of rapamycin. Images were captured, and the percentage of cells that exhibited activated caspase 3/7 enzymes, representing apoptotic activity, in the transfected population was determined. Results indicated that without the rapamycin treatment, the percentage of caspase 3/7-positive cells in total wild type- and E50K optineurin-GFP-overexpressing transfectants was increased by ~1.8–2.5-fold ($p < 0.008$) compared with that in pEGFP-N1-transfected mock controls (Fig. 8*C*). After the rapamycin treatment, the level of apoptosis in optineurin transfectants was declined to within the control limits (Fig. 8*C*).

Transgenic E50K Mouse—The E50K mouse is transgenic, not a knock-in mouse. The transgene was expressed using the chicken β-actin promoter (pCAGGS) with CMV enhancer.

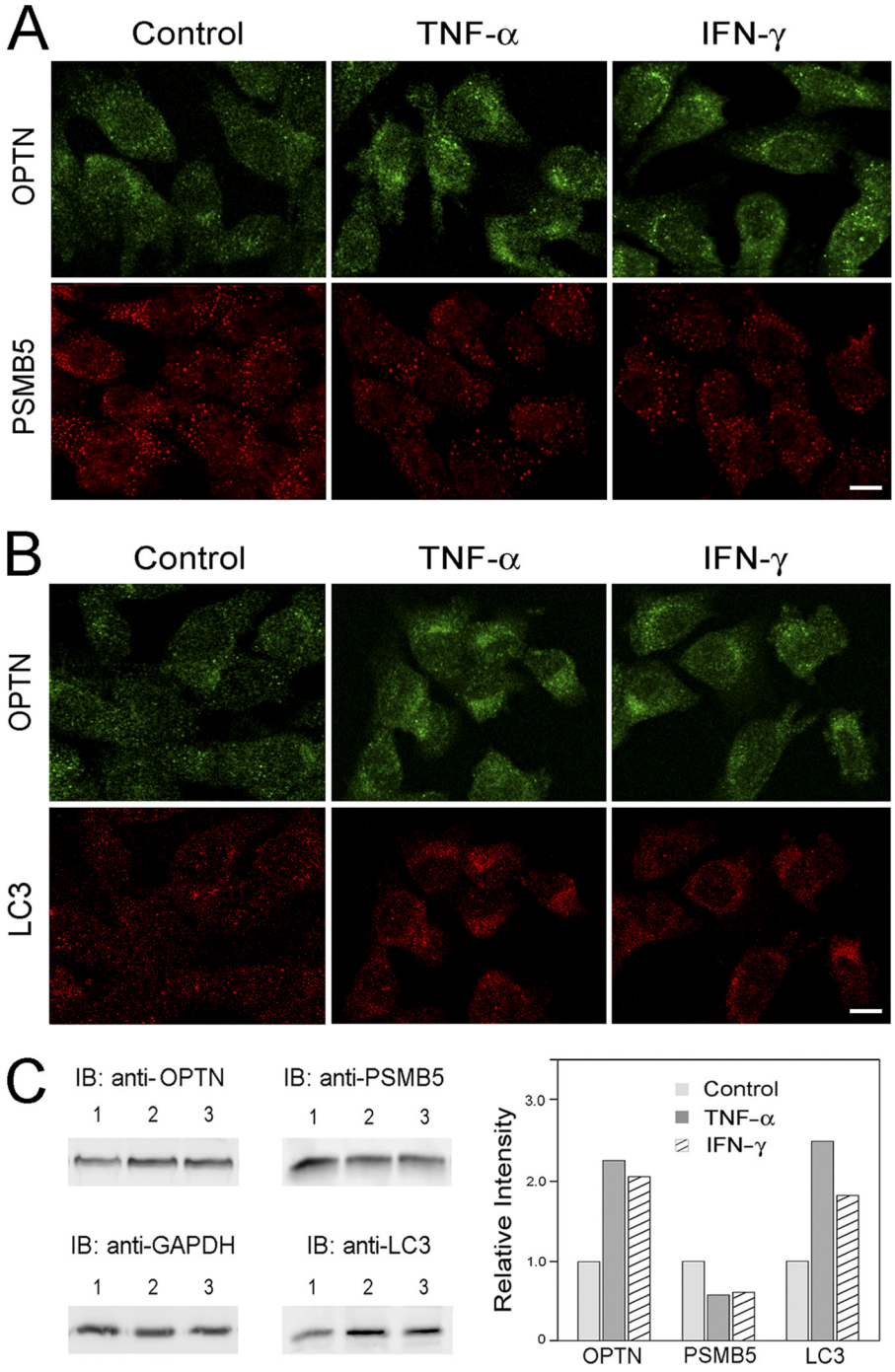

FIGURE 6. *A,* optineurin and PSMB5 immunostaining in RGC5 cells. The cells were treated with TNF-α (100 ng/ml) or IFN-γ (20 ng/ml) for 24 h and were stained with polyclonal rabbit anti-optineurin in *green* or polyclonal rabbit anti-PSMB5 in *red*. The micrographs shown for optineurin and PSMB5 staining were from different specimens. *B,* optineurin and PSMB5 immunostaining in RGC5 cells. The cells were treated with TNF-α or IFN-γ as in *A*. The specimens were double stained with rabbit anti-optineurin in *green* and monoclonal anti-LC3 in *red*. Cells from the same fields are shown for both optineurin and LC3 staining. *Scale bar,* 10 μm. *C,* immunoblotting (*IB*) using anti-optineurin (*OPTN*), anti-PSMB5, anti-LC3, and anti-GAPDH in cells untreated (*lane 1*, control), or treated with TNF-α (*lane 2*) or IFN-γ (*lane 3*) for 24 h. Note that the 18-kDa LC3-I band was barely visible. Only the 16-kDa LC3-II band is shown. As stated earlier, LC3 exists in two forms. LC3-I is cytosolic and LC3-II is lipidated and membrane-bound. The amount of LC3-II is correlated with the extent of autophagosome formation, and an increasing level of LC3-II on immunoblots signals autophagy induction. *Bar graph* depicts the relative intensities (levels) of OPTN, PSMB5, and LC3 compared with untreated controls after normalization to the GAPDH level.

The copy number for the mutant gene was ~12–14 per mouse (41). Although the distribution remained similar, the overall optineurin expression was higher in the retina of E50K transgenic mice compared with the endogenous optineurin expression. The RGC loss and retinal thinning were seen 12 months after birth in the transgenic mice. By 16 months, ~43% of the retinal thickness and ~20% of RGC numbers were reduced (41). Excavation of the optic nerve head was also observed. Apoptotic RGCs were detected in 16- month or older E50K mice. The average intraocular pressure reading for mutant mice was in the normal range of 15 ± 1 mm Hg for all ages examined (41).

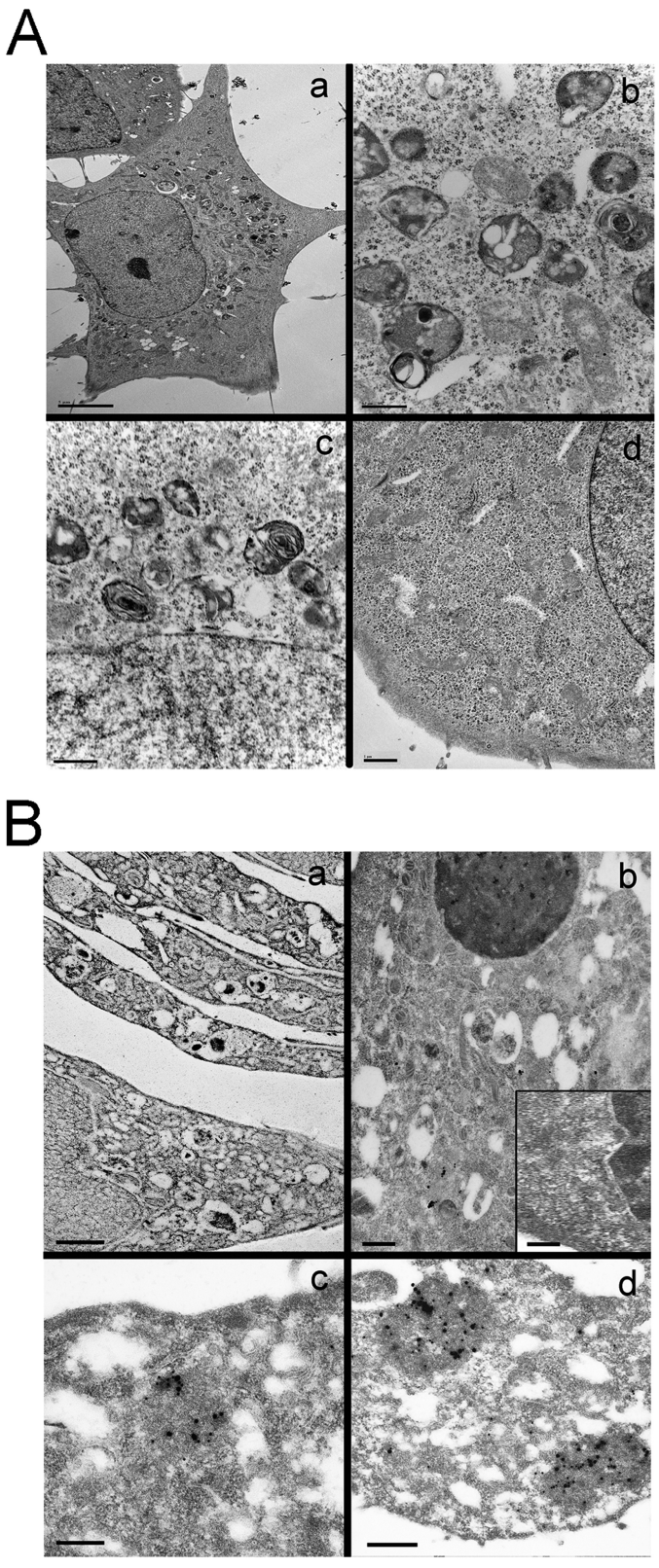

FIGURE 7. *A,* autophagosome- and autolysosome-like structures in optineurin wild type (*panels a* and *b*)- and E50K-GFP (*panel c*)-expressing RGC5 cells. By electron microscopy, the electron dense, organelle-sequestrating, double or multiple membrane structures with diameter averaged between 400 and 600 nm were not observed in GFP-expressing mock-transfected cells (*panel d*). *Scale bar*, 5 μm in *panel a*, 0.5 μm in *panels b* and *c*, and 1 μm in *panel d*. *B*, autophagosome- and autolysosome-like structures are observed in inducible RGC5 cells after DOX induction to express E50K optineurin-GFP (*panels a–d*). A lower magnification micrograph is shown in *panel a* demonstrating those structures in the cytoplasm of several cells. Co-localization of optineurin-GFP (25 nm gold particles) and LC3 (10 nm gold particles) in those structures is seen by immunogold labeling experiments (*panels c* and *d*). The autophagosome- and autolysosome-like structures are barely detected in noninduced controls (*inset* in *panel b*). *Scale bar,* 1 μm in *panel a*, 0.5 μm in *panel b*, and 0.2 μm in *inset*, *panels c* and *d*.

Tissue sections from 12-month-old E50K transgenic mice displayed a fainter staining of PMSB5 but a stronger staining of LC3 in RGCs compared with those from control littermate mice (Fig. 9*B*). Staining with anti-optineurin also yielded a higher intensity in the transgenic tissues as expected (Fig. 9*B*). The enhanced LC3 and reduced PSMB5 staining was also observed in sections from the 4- and 8-month-old transgenic mice (data not shown). Interestingly, no pathology was apparent in the former mice although retinal thickness appeared to be somewhat reduced in the latter.

The staining results in 12-month-old E50K transgenic and normal mice were confirmed by Western blotting of retinal extracts (Fig. 9*C*). By electron microscopy, autophagosome-like structures were demonstrated in RGCs of E50K transgenic eyes (Fig. 9*D*). Quantification analyses indicated that the structures were found in 22 of 33 RGCs examined in transgenic mouse sections, but only in 1 of 23 RGCs in controls.

DISCUSSION

In eukaryotic cells, the ubiquitin-proteasome and autophagy pathways are two major routes for protein clearance (19–21). This study demonstrates that proteasomal inhibition led to an increase in the endogenous optineurin level in neuronal RGC5 and PC12 cells (Fig. 1). On the other hand, autophagic and lysosomal inhibition as well as autophagic activation had little effect. The UPP thus appeared to be the major pathway for endogenous optineurin processing. Autophagy and lysosomes had a rather minor, if any, role. Supporting this conclusion, the endogenous optineurin in RGC5 cells was found ubiquitinated (Fig. 2). UPP has been shown to be the pathway that degrades in a specific manner short lived proteins. The involvement of UPP is therefore consistent with our finding that the half-life of the endogenous optineurin is ~8 h (17). Ubiquitination of the endogenous optineurin also agrees with a previous observation that ^{35}S-labeled, *in vitro*-translated optineurin binds to ubiquitin and is ubiquitinated (16).

Our study further indicates that upon optineurin overexpression or mutation, the proteasome activity in neuronal cells is decreased (Fig. 4) whereas autophagy is induced. The induction of autophagy is evidenced by an increased immunostaining (Fig. 5*A*) for an established autophagic marker LC3 (25), an increased protein level of LC3-II (Fig. 5*B*), the lipidated form of LC3 that inserts into the membrane and correlates with the appearance of LC3-positive autophagosomes (27, 45–47), plus the detection of autophagosome- and autolysosome-like structures in transfected cells (Fig. 6). The overexpressed wild type and E50K optineurins appeared to be processed largely through autophagy, as autophagic activator rapamycin diminishes, whereas the inhibitor 3-MA augments the foci formation (Fig. 8, *A* and *B*).

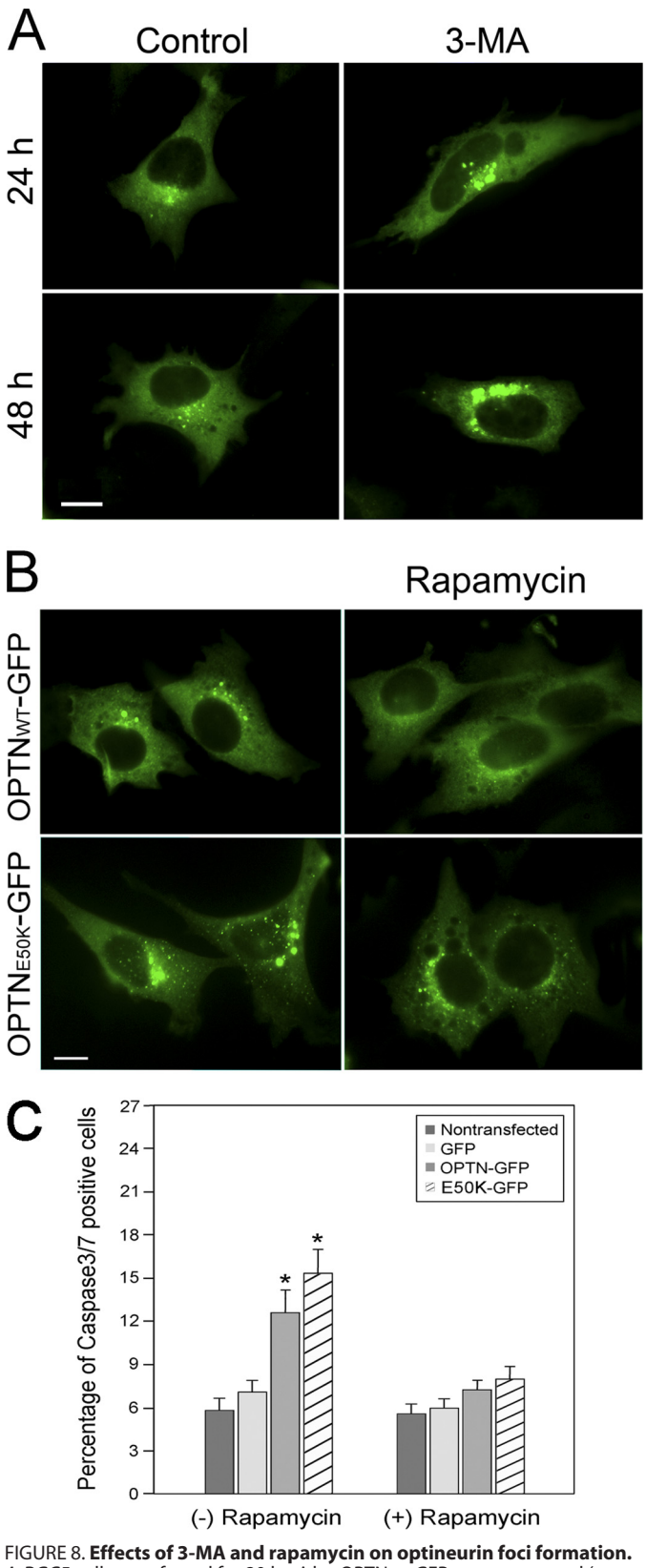

FIGURE 8. **Effects of 3-MA and rapamycin on optineurin foci formation.** *A,* RGC5 cells transfected for 20 h with $pOPTN_{WT}$-GFP were untreated (control) or treated for 24 or 48 h with 3-MA (5 mM), an autophagy inhibitor. Optineurin foci formation was visualized under a Zeiss fluorescence microscope. Note an increased foci formation in 3-MA-treated cells. *B,* RGC5 cells transfected with $pOPTN_{WT}$-GFP and $pOPTN_{E50K}$-GFP were treated for 20 h with rapamycin (2 μM), an autophagy inducer. Note a reduction in foci formation with rapamycin treatment. *Scale bar,* 10 μm. Similar results were also obtained with PC12 cells (data not shown). *C,* percentage of caspase 3/7-positive apoptotic cells in transfected RCG5 cells. The cells transfected for 48 h to express GFP (mock control), wild type optineurin-GFP (OPTN-GFP), and E50K optineurin-GFP (E50K-GFP) were examined by a caspase 3/7 detection kit. One set of cells was treated with 2 μM of rapamycin ((+) *Rapamycin*) for the last 30 h and another was untreated ((−) *Rapamycin*). Images in 20 of 10× fields were captured, and cell counting was performed to determine the total number of transfected cells (*green*) and the number of caspase 3/7-positive transfectants (*green* and *red*). Percentage of caspase 3/7-positive apoptotic transfected cells was calculated. Results from three independent experiments are shown in mean ± S.E. *, $p < 0.008$ compared with GFP controls. Similar patterns were also observed with PC12 cells (data not shown).

A decrease in the PSMB5 level and an increase in the LC3 level were similarly observed in cells treated with TNF-α and IFN-γ (Fig. 6) as well as in inducible cell lines (data not shown). Such *in vitro* changes were likewise observed *in vivo* in E50K transgenic mice. The E50K-overexpressing mice developed phenotype that mimicked the clinical features of NTG patients, including neuropathy of the optic disc and degeneration of the RGCs without an increased intraocular pressure (41). This mouse line thus appears to be the first NTG mouse model. It is notable that the intensity changes of PSMB5 and LC3 staining, although not dramatic, were readily visible (Fig. 9*B*). The protein level changes in the 12-month-old E50K mice were confirmed by Western blotting (Fig. 9*C*). Autophagosome- and autolysosome-like structures were also observed in the E50K specimens (Fig. 9*D*).

It has been documented that when a cytosolic protein is aggregate-prone, it becomes a poor proteasome substrate. One example is α-synuclein, a protein of unknown function and a major component of Lewy bodies (aggregates) observed in Parkinson disease. Mutations of α-synuclein are known to cause autosomal dominant, early onset Parkinson disease. Previous studies have disclosed that both UPP and autophagy are routes for α-synuclein degradation, and that although soluble α-synuclein is cleared by proteasome, the aggregated protein or mutants are preferentially cleared by autophagy (30, 47).

The optineurin degradation hence parallels that described for α-synuclein. The endogenous optineurin seems to be degraded chiefly through the ubiquitin pathway. When optineurin is up-regulated or mutated in neuronal cells, autophagy becomes involved (Figs. 5–7).

The optineurin overexpression characteristics bear similarities to those seen in neurodegenerative diseases, including Alzheimer and Huntington (20, 38, 48). After transfection with wild type or E50K optineurin, the optineurin foci are observed to distribute in the perinuclear region in proximity to the Golgi complex (17, 18, 40). Following precedent of those described for aggresomes, inclusion bodies, or Lewy bodies, the optineurin foci are formed in a microtubule-dependent manner (17, 18). They appear to be LC3-positive (Fig. 5*A*). Also, the proteasome function is impaired (Fig. 4, *C* and *D*) as was seen in neurodegenerative diseases (38, 50, 51). In addition, overexpression of both wild type and E50K optineurin leads to apoptosis in cultured cells (40), and the toxicity can be rescued by rapamycin treatment (Fig. 8*C*). These analogies further underline that glaucoma shares common features with neurodegenerative diseases (52–54).

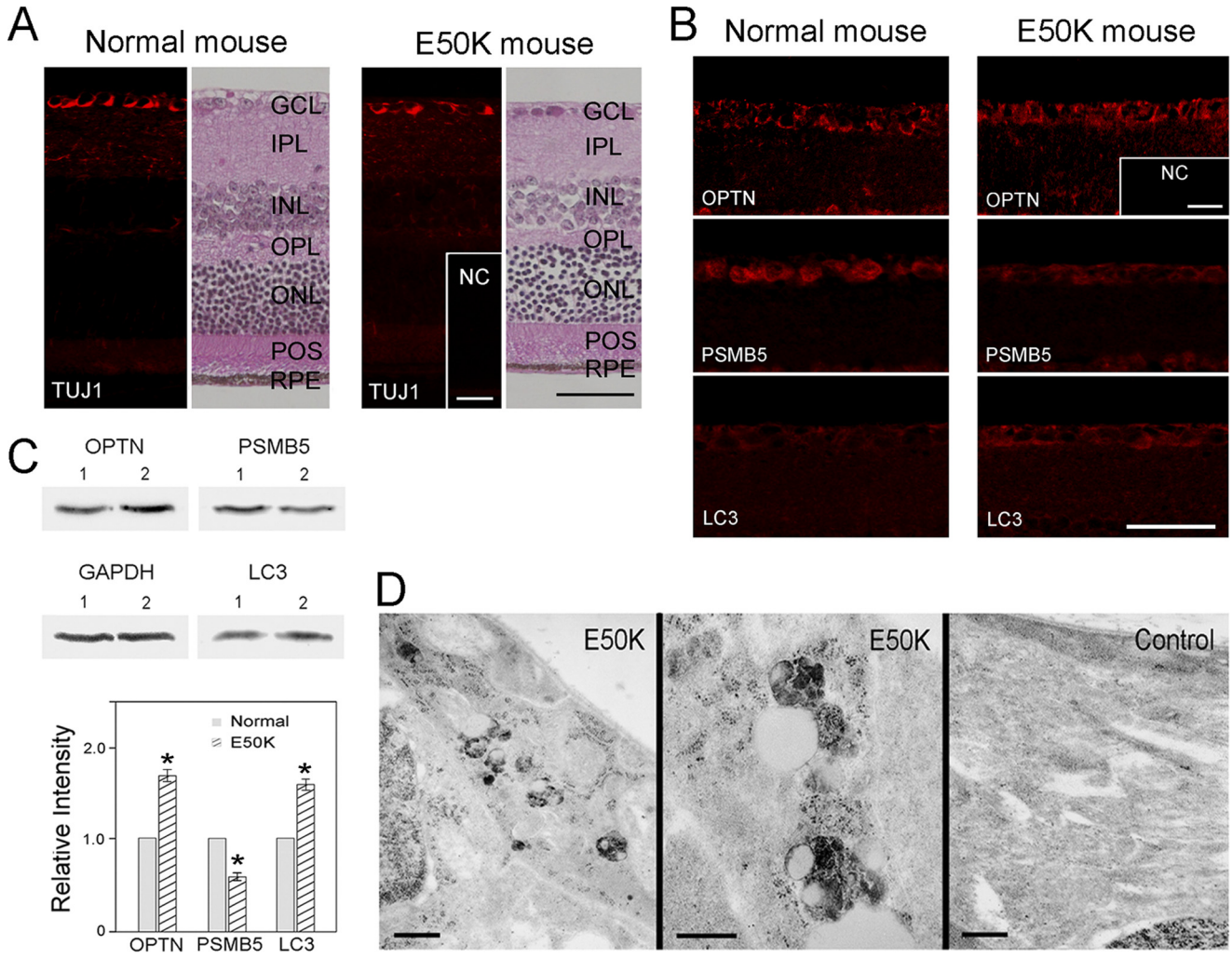

FIGURE 9. *A,* retinal sections from 12-month-old E50K transgenic and normal littermate mice were stained with monoclonal anti-TUJ1 (in *red*) to highlight the RGC layer and with hematoxylin and eosin to demonstrate retinal layers. *GCL,* ganglion cell layer; *IPL*, inner plexiform layer; *INL*, inner nuclear layer; *OPL*, outer plexiform layer; *ONL*, outer nuclear layer; *POS*, photoreceptor outer segments; and *RPE*, retinal pigment epithelium. Note that the retinal thickness is reduced in the E50K transgenic specimen compared with normal control. *Scale bar,* 50 μm. *B,* retinal sections from normal and E50K mice were stained in parallel with polyclonal anti-optineurin, anti-PSMB5, or anti-LC3 (all in *red*). All staining was done using the same antibody concentrations with identical exposure times. As RGCs are the focus of the study, staining in RGCs and the adjacent inner plexiform layer is shown at a higher magnification. Negative controls (*NC*) in which serial sections were stained only with secondary antibodies (for both monoclonal and polyclonal primary antibodies) are shown as *insets*. There was a modest decrease in staining intensity of PSMB5 but an increase in LC3 staining in the RGC layer in transgenic sections compared with normal controls. The optineurin staining was also enhanced in the transgenic mouse. *Scale bar,* 50 μm. *C,* Western blotting for OPTN, PSMB5, LC3, and GAPDH levels in retinal extracts from normal (*lane 1*) or E50K (*lane 2*) mice. Note that for LC3, the 18-kDa LC3-I band was extremely faint. Only the 16-kDa LC3-II band is shown. *Bar graphs*, representing results from three experiments, depict the levels of optineurin, PSMB5, and LC3 relative to normal after normalization to the GAPDH level. *, $p < 0.0053$ compared with normal. *D,* autophagosome- and autolysosome-like structures are observed in RGCs of E50K mouse (*left* and *middle panels*) but are rarely seen in normal littermates (*right panel*). *Bar,* 1 μm in the *left panel*, and 0.5 μm in *middle* and *right panels*.

The role or significance of the foci observed in glaucoma is at present unclear. Interestingly, the roles of inclusion bodies and aggresomes formed in other neurodegenerative diseases are also not clear. As summarized in a number of reviews (21, 26, 55, 56), the inclusion bodies and aggresomes may play a protective role by sequestering toxic, misfolded protein species and providing the cells with an opportunity of delayed protein degradation. They may also inactivate the proteasome and mediate cytotoxicity. Inhibition of proteasome is believed to induce autophagy, which serves as a default mechanism for degradation of the accumulated abnormal proteins. However, when the autophagic clearance system reaches saturation, unable to eliminate the excess proteins, dysregulation or defection may occur, contributing to apoptosis and pathology (26). Supporting this notion, diffuse and abnormal proteins accumulate and aggregate to form inclusions that can disrupt the neural system in Atg5 (autophagy-related gene 5)-deficient mice (57). Also, the protein accumulation and neurodegenerative phenotype could be reverted by activation of the autophagy pathway with a gene therapy approach (58) or infusion of rapamycin (55). It is suggested that there may exist a threshold as a point of divergence between physiological and pathological autophagy (59), and both the physiological and pathological roles of autophagy remain as critically important areas for investigations. Furthermore, inhibition of proteasome function has also been shown to trigger apoptosis (60) depending on cell types and conditions. Defects in the UPP may drive human pathologies, including neurodegenerative

diseases (30), although there have been controversies that still await further clarification (61).

A similar scenario may take place in optineurin-related glaucoma. In this context, it is intriguing that a persistent accumulation of autophagosomes was observed in a recent study (62) in the rat optic nerve following an optic nerve crush injury. The autophagy observed, possibly related to the lesion-induced calcium influx, was thought to be the major pathophysiological mechanism contributing to the ensuing axonal degeneration. It is also of interest that very recently mutations of optineurin are reported to be involved in the pathogenesis of amyotrophic lateral sclerosis (8). Although the role of foci in pathology remains to be precisely defined, an amyotrophic lateral sclerosis case with the E478G optineurin mutation did show optineurin- and ubiquitin-positive cytoplasmic inclusions. Optineurin in addition is linked to Paget disease (9), a condition characterized by focal increases in bone turnover. The osteoclasts in affected bone also contain intranuclear inclusion bodies (63).

There is growing evidence that ubiquitin may be involved in "selective" autophagy (21, 64). It has been shown that ubiquitin-binding receptors such as p62 are required in the process of autophagic clearance of protein aggregates (61, 64). By binding simultaneously to ubiquitin and autophagosome-associated ubiquitin-like LC3, the receptors mediate docking of ubiquitinated protein aggregates to the autophagosome for selective degradation. Optineurin is ubiquitinated, but whether its aggregates are processed through the "selective" autophagy process is currently unknown.

Taken together, this study provides compelling evidence that in normal homeostatic situations, the turnover of endogenous optineurin involves mainly UPP. When optineurin is up-regulated or mutated, the UPP function is compromised, and autophagy comes into play. A decreased PSMB5 level and an induced autophagy were also demonstrated *in vivo* in RGCs of E50K transgenic mice, validating and making relevant the *in vitro* findings.

Optineurin and E50K mutant have been shown to inhibit NF-κB activation (8, 15). Studies from our laboratory reveal that the interaction with Rab8 and transferrin receptor is stronger with the E50K mutant than the wild type optineurin. The mutant also produces a more prominent foci formation (17, 18), more severe fragmentation of the Golgi complex (18), and a higher level of apoptosis (40) than overexpression of the wild type optineurin. Representing a gain-of-function mutation, E50K in addition impairs more dramatically the transferrin trafficking (65). Based on these observations, we surmise that the defective trafficking, deregulated NF-κB signaling, along with fragmentation of the Golgi complex and increased apoptosis may be the underlying bases how the E50K optineurin mutation renders the patients predisposed to the glaucoma pathology. Autophagy, on the other hand, may not be a primary factor in the disease development. This pathway may simply be induced initially as a protective response with buildup of the aggregate-prone mutant protein. Autophagy may contribute to the demise of the cells only when the buildup exceeds the capacity, exacerbating then the disease condition.

It is additionally noteworthy that although the E50K findings have pathological significance, the wild type optineurin overexpression results may also be of physiological relevance. Optineurin, for example, is known to be up-regulated by proinflammatory cytokines TNF-α (14, 36) and IFN (14). Its expression may be heightened to set off adverse consequences upon acute or chronic inflammation and infection. Increases of TNF-α in the retina and the optic nerve head have been associated with glaucomatous conditions (66).

Knowledge of the degradation pathways acting on optineurin can help in the design of novel therapeutic strategies (30). For example, proteasome activity can be promoted by overexpression of proteasome subunit or molecular chaperones, and autophagy can be up-regulated by rapamycin (30), rapamycin plus lithium combination (67), or small molecule autophagy enhancers (49). Future studies will be focused on this translational aspect.

Acknowledgments—We thank Ruth Zelkha for expert imaging and Jack Gibbons, Division of Biological Sciences, for immunogold electron microscopy.

REFERENCES

1. Allingham, R. R., Liu, Y., and Rhee, D. J. (2009) *Exp. Eye Res.* **88,** 837–844
2. Wiggs, J. L. (2007) *Arch. Ophthalmol.* **125,** 30–37
3. Kwon, Y. H., Fingert, J. H., Kuehn, M. H., and Alward, W. L. (2009) *N. Engl. J. Med.* **360,** 1113–1124
4. Wang, N., Chintala, S. K., Fini, M. E., and Schuman, J. S. (2001) *Nat. Med.* **7,** 304–309
5. Rezaie, T., Child, A., Hitchings, R., Brice, G., Miller, L., Coca-Prados, M., Héon, E., Krupin, T., Ritch, R., Kreutzer, D., Crick, R. P., and Sarfarazi, M. (2002) *Science* **295,** 1077–1079
6. Hauser, M. A., Sena, D. F., Flor, J., Walter, J., Auguste, J., Larocque-Abramson, K., Graham, F., Delbono, E., Haines, J. L., Pericak-Vance, M. A., Rand Allingham, R., and Wiggs, J. L. (2006) *J. Glaucoma* **15,** 358–363
7. Aung, T., Rezaie, T., Okada, K., Viswanathan, A. C., Child, A. H., Brice, G., Bhattacharya, S. S., Lehmann, O. J., Sarfarazi, M., and Hitchings, R. A. (2005) *Invest. Ophthalmol. Vis. Sci.* **46,** 2816–2822
8. Maruyama, H., Morino, H., Ito, H., Izumi, Y., Kato, H., Watanabe, Y., Kinoshita, Y., Kamada, M., Nodera, H., Suzuki, H., Komure, O., Matsuura, S., Kobatake, K., Morimoto, N., Abe, K., Suzuki, N., Aoki, M., Kawata, A., Hirai, T., Kato, T., Ogasawara, K., Hirano, A., Takumi, T., Kusaka, H., Hagiwara, K., Kaji, R., and Kawakami, H. (2010) *Nature* **465,** 223–226
9. Albagha, O. M., Visconti, M. R., Alonso, N., Langston, A. L., Cundy, T., Dargie, R., Dunlop, M. G., Fraser, W. D., Hooper, M. J., Isaia, G., Nicholson, G. C., del Pino Montes, J., Gonzalez-Sarmiento, R., di Stefano, M., Tenesa, A., Walsh, J. P., and Ralston, S. H. (2010) *Nat. Genet.* **42,** 520–524
10. Li, Y., Kang, J., and Horwitz, M. S. (1998) *Mol. Cell. Biol.* **18,** 1601–1610
11. Rezaie, T., and Sarfarazi, M. (2005) *Genomics* **85,** 131–138
12. Kroeber, M., Ohlmann, A., Russell, P., and Tamm, E. R. (2006) *Exp. Eye Res.* **82,** 1075–1085
13. De Marco, N., Buono, M., Troise, F., and Diez-Roux, G. (2006) *J. Biol. Chem.* **281,** 16147–16156
14. Schwamborn, K., Weil, R., Courtois, G., Whiteside, S. T., and Israël, A. (2000) *J. Biol. Chem.* **275,** 22780–22789
15. Sudhakar, C., Nagabhushana, A., Jain, N., and Swarup, G. (2009) *PLoS ONE* **4,** e5114
16. Zhu, G., Wu, C. J., Zhao, Y., and Ashwell, J. D. (2007) *Curr. Biol.* **17,** 1438–1443

17. Ying, H., Shen, X., Park, B., and Yue, B. Y. (2010) *PLoS One* **5,** e9168
18. Park, B. C., Shen, X., Samaraweera, M., and Yue, B. Y. (2006) *Am. J. Pathol.* **169,** 1976–1989
19. Glickman, M. H., and Ciechanover, A. (2002) *Physiol. Rev.* **82,** 373–428
20. McCray, B. A., and Taylor, J. P. (2008) *Neurosignals* **16,** 75–84
21. Kirkin, V., McEwan, D. G., Novak, I., and Dikic, I. (2009) *Mol. Cell* **34,** 259–269
22. Mukhopadhyay, D., and Riezman, H. (2007) *Science* **315,** 201–205
23. Mizushima, N. (2007) *Genes Dev.* **21,** 2861–2873
24. Meijer, A. J., and Codogno, P. (2009) *Crit. Rev. Clin. Lab. Sci.* **46,** 210–240
25. Eskelinen, E. L. (2005) *Autophagy* **1,** 1–10
26. Bao, X. H., Naomoto, Y., Hao, H. F., Watanabe, N., Sakurama, K., Noma, K., Motoki, T., Tomono, Y., Fukazawa, T., Shirakawa, Y., Yamatsuji, T., Matsuoka, J., and Takaoka, M. (2010) *Int. J. Mol. Med.* **25,** 493–503
27. Mizushima, N., Yoshimori, T., and Levine, B. (2010) *Cell* **140,** 313–326
28. Levine, B., and Kroeme, G. (2008) *Cell* **132,** 27–42
29. Mizushima, N., Levine, B., Cuervo, A. M., and Klionsky, D. J. (2008) *Nature* **451,** 1069–1075
30. Rubinsztein, D. C. (2006) *Nature* **443,** 780–786
31. Krishnamoorthy, R. R., Agarwal, P., Prasanna, G., Vopat, K., Lambert, W., Sheedlo, H. J., Pang, I. H., Shade, D., Wordinger, R. J., Yorio, T., Clark, A. F., and Agarwal, N. (2001) *Brain Res. Mol. Brain Res.* **86,** 1–12
32. Van Bergen, N. J., Wood, J. P., Chidlow, G., Trounce, I. A., Casson, R. J., Ju, W. K., Weinreb, R. N., and Crowston, J. G. (2009) *Invest. Ophthalmol. Vis. Sci.* **50,** 4267–4272
33. Greene, L. A., and Tischler, A. S. (1976) *Proc. Natl. Acad. Sci. U.S.A.* **73,** 2424–2428
34. Choi, J., Miller, A. M., Nolan, M. J., Yue, B. Y., Thotz, S. T., Clark, A. F., Agarwal, N., and Knepper, P. A. (2005) *Invest. Ophthalmol. Vis. Sci.* **46,** 214–222
35. Park, B. C., Tibudan, M., Samaraweera, M., Shen, X., and Yue, B. Y. (2007) *Genes Cells* **12,** 969–979
36. Vittitow, J., and Borrás, T. (2002) *Biochem. Biophys. Res. Commun.* **298,** 67–74
37. Caballero, M., Liton, P. B., Challa, P., Epstein, D. L., and Gonzalez, P. (2004) *Biochem. Biophys. Res. Commun.* **323,** 1048–1054
38. Bence, N. F., Sampat, R. M., and Kopito, R. R. (2001) *Science* **292,** 1552–1555
39. Bence, N. F., Bennett, E. J., and Kopito, R. R. (2005) *Methods Enzymol.* **399,** 481–490
40. Koga, T., Shen, X., Park, J. S., Qiu, Y., Park, B. C., Shyam, R., and Yue, B. Y. (2010) *Am. J. Pathol.* **176,** 343–352
41. Chi, Z. L., Akahori, M., Obazawa, M., Minami, M., Noda, T., Nakaya, N., Tomarev, S., Kawase, K., Yamamoto, T., Noda, S., Sasaoka, M., Shimazaki, A., Takada, Y., and Iwata, T. (2010) *Hum. Mol. Genet.* **19,** 2606–2615
42. Huang, Y., Li, Z., van Rooijen, N., Wang, N., Pang, C. P., and Cui, Q. (2007) *Exp. Eye Res.* **85,** 659–666
43. Eskelinen, E. L. (2008) *Autophagy* **4,** 257–260
44. Martinez-Vicente, M., Talloczy, Z., Wong, E., Tang, G., Koga, H., Kaushik, S., de Vries, R., Arias, E., Harris, S., Sulzer, D., and Cuervo, A. M. (2010) *Nat. Neurosci.* **13,** 567–576
45. Klionsky, D. J., Cuervo, A. M., and Seglen, P. O. (2007) *Autophagy* **3,** 181–206
46. Mizushima, N., and Yoshimori, T. (2007) *Autophagy* **3,** 542–545
47. Webb, J. L., Ravikumar, B., Atkins, J., Skepper, J. N., and Rubinsztein, D. C. (2003) *J. Biol. Chem.* **278,** 25009–25013
48. Pan, T., Kondo, S., Le, W., and Jankovic, J. (2008) *Brain* **131,** 1969–1978
49. Renna, M., Jimenez-Sanchez, M., Sarkar, S., and Rubinsztein, D. C. (2010) *J. Biol. Chem.* **285,** 11061–11067
50. Mayer, R. J. (2003) *Drugs News Perspect.* **16,** 103–108
51. Ross, C. A., and Pickart, C. M. (2004) *Trends Cell Biol.* **14,** 703–711
52. McKinnon, S. J. (2003) *Front. Biosci.* **8,** s1140–1156
53. Gupta, N., and Yücel, Y. H. (2007) *Curr. Opin. Ophthalmol.* **18,** 110–114
54. Normando, E. M., Coxon, K. M., Guo, L., and Cordeiro, M. F. (2009) *Exp. Eye Res.* **89,** 446–447
55. García-Arencibia, M., Hochfeld, W. E., Toh, P. P., and Rubinsztein, D. C. (2010) *Semin. Cell Dev. Biol.* **21,** 691–698
56. Glick, D., Barth, S., and Macleod, K. F. (2010) *J. Pathol.* **221,** 3–12
57. Hara, T., Nakamura, K., Matsui, M., Yamamoto, A., Nakahara, Y., Suzuki-Migishima, R., Yokoyama, M., Mishima, K., Saito, I., Okano, H., and Mizushima, N. (2006) *Nature* **441,** 885–889
58. Spencer, B., Potkar, R., Trejo, M., Rockenstein, E., Patrick, C., Gindi, R., Adame, A., Wyss-Coray, T., and Masliah, E. (2009) *J. Neurosci.* **29,** 13578–13588
59. Cherra, S. J., 3rd, Dagda, R. K., and Chu, C. T. (2010) *Neuropathol. Appl. Neurobiol.* **36,** 125–132
60. Jana, N. R., Zemskov, E. A., Wang, Gh., and Nukina, N. (2001) *Hum. Mol. Genet.* **10,** 1049–1059
61. Matsuda, N., and Tanaka, K. (2010) *J. Alzheimers Dis.* **19,** 1–9
62. Knöferle, J., Koch, J. C., Ostendorf, T., Michel, U., Planchamp, V., Vutova, P., Tönges, L., Stadelmann, C., Brück, W., Bähr, M., and Lingor, P. (2010) *Proc. Natl. Acad. Sci.* **107,** 6064–6069
63. Ralston, S. H. (2008) *Bone* **43,** 819–825
64. Wong, E., and Cuervo, A. M. (2010) *Nat. Neurosci.* **13,** 805–811
65. Park, B., Ying, H., Shen, X., Park, J. S., Qiu, Y., Shyam, R., and Yue, B. Y. (2010) *PLoS One* **5,** e11547
66. Tezel, G. (2008) *Prog. Brain Res.* **173,** 409–421
67. Sarkar, S., Krishna, G., Imarisio, S., Saiki, S., O'Kane, C. J., and Rubinsztein, D. C. (2008) *Hum. Mol. Genet.* **17,** 170–178